Journal of Materials and Applications 2024;13(1):1-10
https://doi.org/10.32732/jma.2024.13.1.1

Evaluation of Mechanical Properties of Self-cured, Heat-cured, and Photosensitive 3D Printing Resins After the Addition of Silica Nanoparticles

Cristiane Maria Boniatti Mussatto[1], Elisa Magno Nunes de Oliveira[2], Karthikeyan Subramani[3], Eduardo Gonçalves Mota[1], Ricardo Meurer Papaléo[2]

1. Department of Dentistry School of Health and Life Sciences, Brazil
2. Interdisciplinary Center of Nanoscience and Micro-Nanotechnology; School of Technology, Pontifical Catholic University of Rio Grande do Sul, Porto Alegre, Brazil
3. Department Advanced Education in Orthodontics and Dentofacial Orthopedics, College of Dental Medicine, Roseman University of Health Sciences, Henderson, USA
E-mail: crisboni2018@gmail.com

Received: 6 January 2024; Accepted: 5 March 2024; Available online: 30 May 2024

Abstract: This study evaluated investigate the addition of silica nanoparticles in autopolymerizable resin and into liquid resin for 3D printing and compare them with CAD-CAM blocks and thermopolymerizable resin, regarding flexural strength and surface roughness. Eight groups (n=12) were created according to the types of materials: autopolymerizable resin (G1-G4), photosensitive resin for 3D printing (G5-G6), PMMA block (G7) and thermopolymerizable resin (G8). Functionalized silica nanoparticles (0.5-1.5 wt%) were added in groups G2-G4 and G6. Mechanical flexural strength, surface roughness and morphological analysis were carried out to evaluate the properties of the samples. One-way ANOVA, followed by Tukey's post-hoc test, was used to evaluate the data. The average surface roughness was higher in group G7 and lower in the G8 group, with a statistical difference ($p < 0.001$). The G8 and G1-G4 showed no significant difference in surface roughness. The G5 and G6 presented surface roughness higher than that recommended by Borchers and Bollen (Ra=0.2 µm). The incorporation of nanoparticles into self-polymerizing acrylic resins negatively affected the mechanical properties of the material, reducing flexural strength. The G5 and G6 demonstrated the lowest flexural strength ($p<0.001$), presenting values lower than those recommended by ISO (σ >60 MPa) regardless of the incorporation or not of silica nanoparticles. The G7 presented the highest flexural strength value followed by the G8. Within the limits of this study, it may be concluded that the addition of silica nanoparticles did not improve the flexural strength the G6 and also affected negatively the mechanical properties of self-polymerizing acrylic resins.
Keywords: PMMA; Silica nanoparticles; CAD/CAM; 3D print.

1. Introduction

The fabrication of crowns, myorelaxing plates and indirect restorations from polymeric resins is of utmost importance in many different fields of odontology, from prosthodontics and restorations to oral implantology or orthodontics[1,2]. Until recently in dentistry, the use of molds and the computer-aided design (CAD) and computer-aided manufacturing (CAM) were the most common techniques for manufacturing. CAD-CAM uses milling, grinding, drilling, and turning by means of specific tools and is classified as a subtractive technique. Thus the material loss is high and limits the number of objects to be milled with the same block material [2,3]. CAD/CAM technology brings advantages, such as digital model impressions and the use of virtual articulators [4], but is still considered costly and requires highly trained personnel. Another advantage of this technology is decreased patient dwell time in the dental chair and increased patient comfort by eliminating conventional molding procedures [2,5–12].

In 1986, Charles Hull introduced and patented the first 3D printing known as stereolithography (SLA). Since then, technologies have been developed and their use expanded. Nowadays, with the expiration of patents, the development of new 3D printing technologies has increased and the production costs decreased considerably [1,2]. The 3D printing additive manufacturing process can spare material and produce more complex geometries on demand. It still has disadvantages, such as high costs and postprocessing time [2,3]. 3D printing can be applied to plastic, metal, ceramic, concrete and other building materials; however this technology is still predominantly used for the production of polymeric parts and models [13]. Several possibilities of 3D printing using different polymers

have already been demonstrated in dentistry, and the technique is rapidly approaching everyday dental practice as a highly flexible processing technique [2,3].

The main 3D printing processes described in the literature are: stereolithography (SLA); digital light processing (DLP); material jetting (MJ); fused deposition modeling (FDM); binder jetting (BJ); and powder-based printing. Stereolithography (SLA) and digital light processing (DLP) are light curing technologies, in which the materials used are photoresist resins [1]. SLA and DLP are the most advanced 3D printing technologies in dentistry. [3] SLA is one of the earliest practical 3D printing technologies. There are two ways to move the printing platform in SLA technology: the top-down and the bottom-up movement of the platform. In the platform-bottom-up approach, the platform is submerged at the bottom of the resin tank, and in the gap between the platform and the bottom only a single layer of resin is spread [2]. In SLA 3D printing, the light is radiated by a laser with selective exposure. The printing speed is lower, but the accuracy is much higher. The total cost involved is also slightly higher. The main difference between DLP and SLA is the light source, since DLP uses a shallow resin light source and a digital light projector located underneath the resin tank curing entire layers of resin at once. The printing speed the DLP is higher, the whole cost involved is lower [1].

The most common application of 3D printing technology in dentistry is the creation of working and diagnostic models and guides for surgery, occlusal devices followed by a variety of implantable devices that can help dentists provide patients with more predictable and less costly procedures [2]. Myorelaxing plates made of polymethyl methacrylate, considered the gold-standard material, are giving way to CAD/CAM technology (PMMA blocks and 3D printing resins). 3D printing resins are polymerized layer by layer, decreasing the manufacturing time and can be performed in the clinic, minimizing laboratory steps. [14].

New technologies end up requiring an adaptation of existing materials or the development of new materials [14]. In this direction, nanoparticles (NPs) incorporated into polymers are promising materials to enhance the properties (surface roughness and flexural strength) of dental resins [15,16]. Many researchers have studied the effect of different additive constituents on material conversion and properties in order to improve printed materials [2,17–20]. For example, silica NPs have been incorporated into self-curing resin to improve mechanical properties, but there were no significant improvements in flexural strength and hardness [21,22]. These studies suggested that the dispersion and aggregation of silica NPs may cause an adverse effect on flexural strength. The use of coupling agents to link the nanoparticles into the resin structure may improve performance. Silanes, such as 3-methacryloxypropryltrimethoxysilane (MPS), have been tested with good results, since the silane groups on the surface of NPs copolymerize with the methacrylate polymer matrix, promoting bonding with the resin and providing superior performance for the composites [22–26]. Further studies are necessary on materials for CAD/CAM and 3D printing technologies capable of producing extensive and long provisional rehabilitative treatments with adequate flexural strength, hardness, and smoothness especially in patients with parafunctional habits. The aim of this study was to investigate the addition of functionalized-silica nanoparticles in self-cured resin and liquid resin for 3D printing and compare them with PMMA blocks and heat-cured resin, regarding flexural strength and surface roughness for fabrication of crowns, myorelaxing plates and indirect restorations.

2. Materials and Methods

2.1 Materials

The reagents ethanol, ammonium hydroxide (28%), tetraethyl orthosilicate (TEOS), 3- trimethoxysiylpropyl methacrylate (MPS), cyclohexane and n-propylamine were purchased from Sigma-Aldrich. JET Clássico resin (Artigos Odontológicos Clássico Ltda, São Paulo, Brazil) was used to prepare the self-curing samples. For printing, photosensitive resin from Cosmos (Yller Biomaterials reference1030 batch 00005975) was employed. The polymethylmethacrylate (PMMA) block specimens were prepared from Vipiblock (Vipi- Pirassununga, São Paulo, Brazil). For the thermopolymerizing acrylic resin specimens, Clássico- Acrylic Thermopolymerizing resin (Artigos Odontológicos Clássico Ltda São Paulo, Brazil) was used. Two impression materials were used: 3M Empress XT (3M ESPE Germany) for self-curing acrylic resin and Zetalabor (Zhermach Italy) for Thermopolymerizing acrylic resin.

2.2 Synthesis and characterization of the silica nanoparticles

The functionalized NPs were previously synthesized and characterized according to Mussatto et al. 2020 [22]. Briefly, ultrapure water (6.2 mol), ethanol (1.9 mol), and ammonium hydroxide (0.62 mol) were mixed in a reactor under magnetic stirring. In a separation funnel, TEOS (22.4 mmol) and ethanol (0.17 mol) were also mixed and added to the previous solution. The reaction system was kept under constant magnetic stirring for 4 h, at 25 °C. The NPs dispersion was centrifuged at 3000 rpm for 30 min and subsequently washed with ethanol. The remaining NP powder was dried in an oven at 120 °C. The SiO_2-NPs were then functionalized with MPS, following the adapted protocol from Karabela [26]. In a reactor, 1.0 g of SiO_2-NPs was mixed with cyclohexane (0.18 mol), n-propylamine (0.34 mmol), and MPS (2.8 mmol) and kept under magnetic stirring for 30 min. The mixture was

placed under reflux at 60 °C, for 30 min and subsequently dried in rotary evaporator at 60 °C. The remaining solid was dried in an oven at 80 °C, for 4 h. The silanized nanoparticles (s-SiO_2-NPs) were stored in a desiccator. The mean diameter measured by scanning microscopy (SEM-FEG, Inspect-F50 model, FEI) were 140 ± 33 nm for the s-SiO_2-NPs, and their absorption spectra in infrared region (FTIR-Spectrum One, PerkinElmer) showed the stretching vibration from carbonyl groups (C=O) of methacrylate groups, indicating the NPs functionalization (details in reference [22]).

2.3 Group division

Eight groups (G1-G8) were formed using self-curing resin, impression resin, PMMA block for milling and heat-curing resin, with or without addition of s-SiO_2-NPs, as presented in Table 1.

Table 1. Groups description according to type, concentration, and method incorporation of s-SiO_2-NPs into the different resins

Groups	Type	s-SiO_2-NP wt.%	Incorporation
G1 (ctrl)	Self-curing resin	-	-
G2	Self-curing resin	0.5	monomer
G3	Self-curing resin	1.0	monomer
G4	Self-curing resin	1.5	monomer
G5 (ctrl)	Resin for printing	-	-
G6	photosensitive resin for 3D printing	1.0	monomer
G7 (ctrl)	PMMA Block	-	-
G8	Thermopolymerizable Resin	-	-

2.4 Sample Preparation

All samples were prepared in a rectangular shape with dimensions of (64 x 10 x 3.3 ± 2 mm) as recommended by ISO 20795-1:2013 [27]. There were three different procedures to mold the samples: pouring and curing the resins in silicone molds, direct printing, and milling of a solid block. To prepare the silicone molds for the self-curing resins, four units of metal stripes (64 x10 x 3.3 mm) separated by 1 cm were placed inside a plastic box (9 x 9 x 15 cm). Then, regular body addition silicone was injected over the metal. A glass slab and a 1 kg weight were overlaid on top until the end of curing time, producing the silicone templates shown in Fig. 1A.

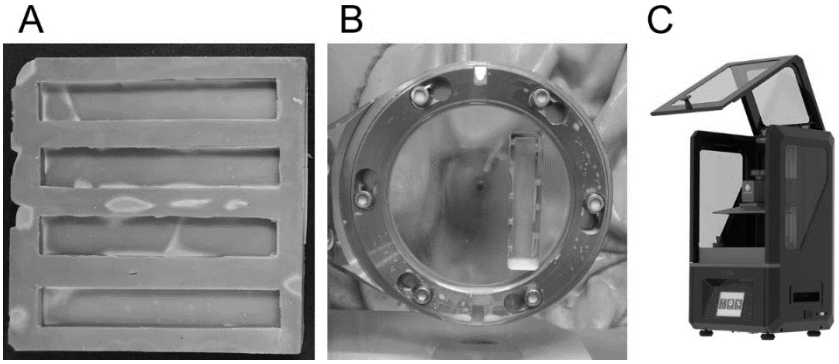

Fig. 1. Addition silicone mold (A), Milling machine BR3D (Tecnodrill) (B), and Anycubic Photon S (C)

Samples from groups G1 to G4 were prepared following the standard procedure for self-cured dental resins. The nanocomposites for groups G2, G3 and G4 were prepared by adding s-SiO_2-NPs into the monomer (liquid), according to the weight percentage described in the Table 1. To disperse the NPs, the mixture was stirred in an ultrasonic bath (Digital Ultrasonic Cleaner - 4810, Gnatus) for 3 min, inside of glass container (Paladon) with water at 7 °C to decrease the polymerization time of the acrylic resin. Then, the polymer was added to the monomer and kept for 1 min. A plastic syringe was loaded with 20 mL of the final acrylic resin and used to fill the silicone mold. A 4 mm-thick glass plate was placed on top of the silicone mold with a weight of 1 kg, to avoid the formation of air bubbles. The initial setting of the self-curing process is fast (~ 5 min) and the entire process the self-curing was completed in about 20 min. After curing, each sample was rectified (aligned, defects corrected) in a milling machine (Clever) in three equal stripes of 64 x 10 x 3.3 ± 2 mm.

Printed samples G5 and G6 were based on a photosensitive resin from Cosmos (Yller Biomaterials reference1030 batch 00005975) and prepared using the Anycubic Photon S printer (Fig. 1B). The 3D printer features a high-resolution Ultra HD 2K LCD screen, with LED light of wavelength around 405 nm to cure photopolymers layer by layer. The printing process begins when the build platform descends into the resin tank

and the UV light from the digital projector cures the resin. The Tinkercad software was used to make the design (STL) of the rectangular samples 64 x 10 x 3.3 mm. All the impressions were made horizontally (0 degree angle). In the group G5, 50 mL of the resin was added to the printer tray. In the group G6, initially 1 wt.% of s-SiO_2-NPs was added to 50 mL of Anycubic resin in a glass container, and the mixture was stirred in an ultrasonic cleaner for 3 min. The printer tray was then loaded with the mixture for printing. After printing, the samples were cleaned twice in an ethanol bath for 5 min and dried. Post-polymerization of the samples was carried out in a 50W UV chamber for 10 min. The specimens were sanded according to the recommendations of ISO2013 [27].

Group G7 samples were prepared in a BR3D milling machine (Tecnodrill Novo Hamburgo, RS, Brasil) (Fig. 1C) from a PMMA disc (Vipiblock São Paulo, Brazil). To produce the samples of group G8 (thermosetting resin) a silicone mold (Zetalabor condensation silicone) was placed in a metal muffle. After pouring the resin, the muffle was closed, compressed by means of a hydraulic press, and the polymerization cycle started at 120 °C for 2 hours.

Samples from the groups G1 to G6 and G8 were polished in a Struers polishing machine (DPU-10, Panambra, Brazil), under constant refrigeration, using metallographic sandpapers in a sequence (P500, P1000, P1200) recommended by ISO (ISO 20795-1-2013) [27]. Samples from Group G7 (Vipiblock), were cleaned and disinfected with alcohol and subsequently cut and polished with polishing kit (microdont) as indicated by the manufacturer.

2.5 Surface morphology, elemental composition, and roughness

The morphology and elemental composition of the samples were evaluated by scanning electron microscopy and energy dispersive spectroscopy (EDS) analysis in a Inspect-F50 SEM-FEG (FEI). The surface roughness (Ra, arithmetical mean height) of each specimen was measured using a digital profilometer (SJ 201 Mitutoyo, Japan), attached to a metal base to eliminate unwanted vibrations and assure reading fidelity. The profiler moved the diamond stylus across 0.25 mm of the sample under a constant load. Three readings per specimen were acquired.

2.6 Flexural strength test

All samples for the flexural strength test were prepared following ISO 20795-1: 2013 [27]. The samples were immersed in a water bath at 37 °C for 50 ± 2 h, prior to testing. After, the samples were randomly chosen using Excel software (Office-Microsoft), and each specimen was placed symmetrically with the flat surface on the test fixtures. The specimens were tested until fracture in a universal testing machine (EMIC DL - 2000) at a speed of 5 mm/min and using a load cell of 50 Kgf. The flexural strength of each specimen was calculated in megapascals (MPa), according to the formula: $FS=3FL/2bh^2$, where FS represents the flexural strength, F is the maximum load exerted on the specimen in Newtons (N), L is the distance between the supports (50 mm), b is the specimen width (mm), and h is the specimen thickness (mm). The ultimate strength of the specimens was recorded.

2.7 Statistical analysis

Data were first subjected to the Kolmogorov-Smirnova normality test, and then evaluated by one-way ANOVA, followed by Tukey's post-hoc test, when significant differences were found between groups. The significance level was considered $p < 0.05$. Data were analyzed by SPSS Statistic (v22.0, IBM Corp Armonk, NY).

3. Results

3.1 Sample morphology and roughness

Typical surface morphology of samples from groups G1 to G8 can be seen in the electron microscopy images shown in Figs. 2 and 3.

The insets depict the respective EDS spectra, note that Au was used for metallization of the samples. Pure self-cured acrylic samples (G1, Fig. 2A) showed relatively smooth surfaces with a few scratches, possibly due to sample processing. The EDS spectrum did not indicate the presence of Si, as expected. The micrographs from sample G2 showed a distribution of holes on the surface, also attributed to sample preparation (Fig. 2B). Although the EDS spectrum indicates the presence of the element Si in the sample, individual NPs are not clearly identified. The micrographs of samples from G3 and G4, on the other hand, indicate the presence of particulate structures, possibly due to NPs agglomerates. The presence of Si is also confirmed in the EDS spectra. The micrographs of samples from the groups G5-G8 are shown in Fig. 3. The stripes seen in Figs. 3A and B are characteristic of the layer-by-layer mode of the 3D printing. In the case of the sample G6 prepared with the nanocomposite ink (Fig. 3B) clusters of particles or grains are seen also on the surface of the sample. The EDS spectrum of G6 confirmed the presence of silicon in the sample. For the pure printing ink (G5) neither the particulate structure, nor the Si signal are seen in the samples, as expected. The surface morphology of samples made from blocks (G7) is homogeneous. For G8 a distribution of scratches is seen on the surface.

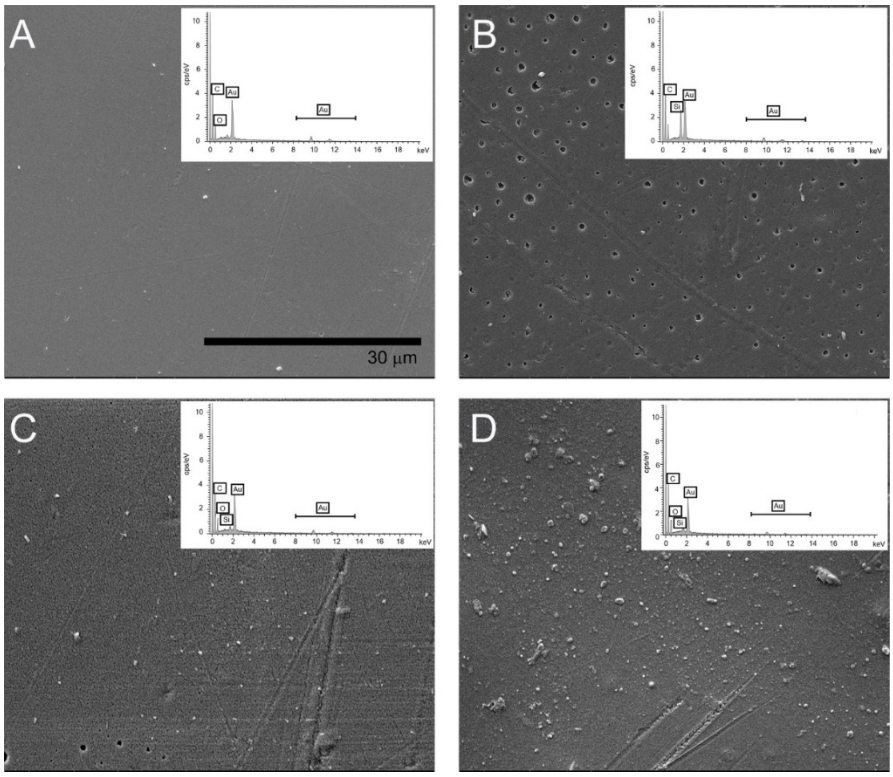

Fig. 2. Scanning electron microscopy micrographs of self-cured acrylic resin. Unmodified self-cured resin sample G1 (A), sample from group G2 (0.5 wt.% of s-SiO_2-NPs incorporated in the monomer) (B), sample from group G3 (1 wt.% of s-SiO_2-NPs incorporated in the monomer) (C), and sample from group G4 (1.5 wt.% of s-SiO_2-NPs incorporated in the monomer) (D). All images were collected at equal magnification and scale bar in one application for all frames. Inner: energy dispersive spectroscopy (EDS) of respectively groups.

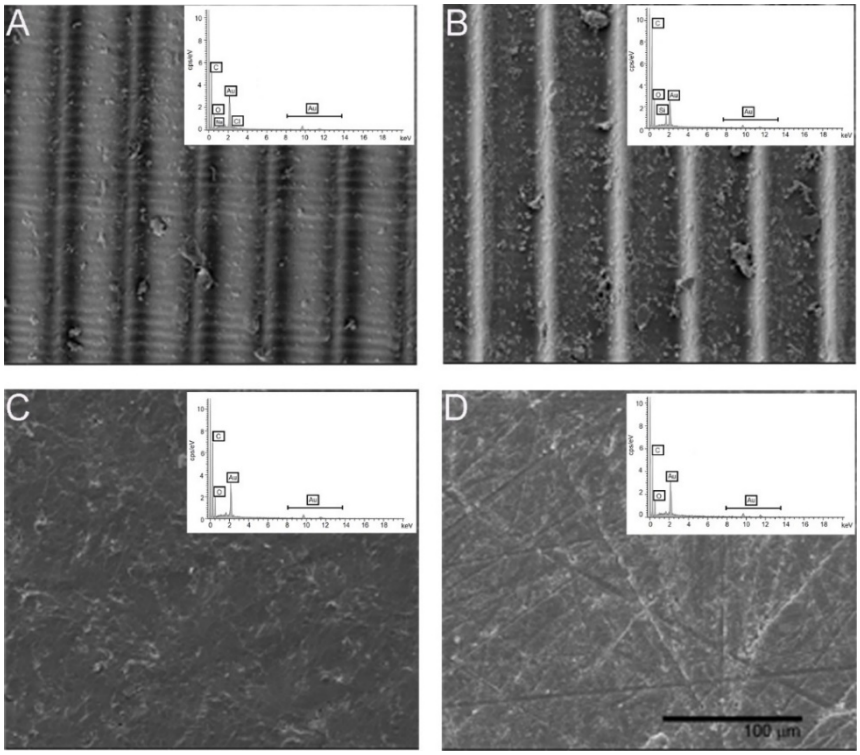

Fig. 3. Scanning electron microscopy micrographs of impression resin, PMMA block and thermosetting resin. Sample of group G5 (unmodified impression resin) (A), sample of group G6 (1 w% s-SiO_2-NPs incorporated in the photosensitive resin for 3D printing) (B), sample of group G7 (unmodified PMMA block) (C), and sample of group G8 (unmodified thermosetting resin) (D). All images were collected at equal magnification and scale bar in one application for all frames.

The mean surface roughness of samples from groups G1-G8 are shown in Fig. 4.

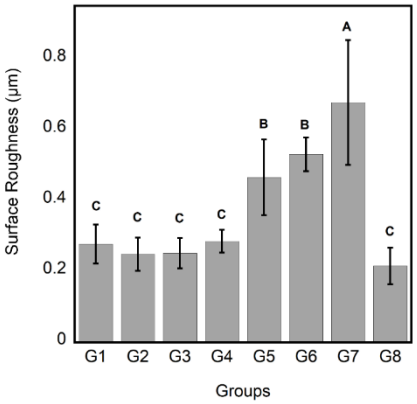

Fig. 4. Mean surface roughness of samples from groups G1-G8. Different letters represent statistical difference at 5% level by Tukey's test.

Surface roughness among the groups of self-cured acrylic resins (G1-G4) was similar. Differences are within the uncertainties of the measurements and were not statistically significant. There is, however, a trend of the mean roughness to increase with increasing filler content (Table 2), perhaps due the silanized silica NPs getting interposed between the polymer chains.

Table 2. Flexural strength and surface roughness of G1-G8 samples

Samples	Surface roughness (µm)	Flexural strength (MPa)
G1	0.277 ± 0.05	71.95 ± 7.6
G2	0.249 ± 0.04	71.88 ± 11.1
G3	0.252 ± 0.04	67.77 ± 7.4
G4	0.285 ± 0.03	67.55 ± 6.8
G5	0.460 ± 0.03	35.46 ± 6.8
G6	0.530 ± 0.04	35.08 ± 7.1
G7	0.677 ± 0.17	105.86 ± 12.5
G8	0.216 ± 0.05	88.52 ± 12.2

Yet, the effect is small. This trend is also seen in the printed samples, with samples from G6 (with addition of 1 wt.% of s-SiO_2-NPs) displaying slightly increased surface roughness compared to G5. The highest value of surface roughness occurred in the PMMA block G7 (0.677 µm) and the lowest value for the G8 (0.216 µm) with $p < 0.001$. G8, however, showed no significant differences when compared to groups G1, G2, G3 and G4. The roughness of 3D printing resin groups (G5 and G6) also differed statistically from all other groups but showed no significant difference between them. The 3D printing resins showed surface roughness larger than recommended by Bollen et al. and Borchers et al. (which is Ra 0.2 µm) [28,29] and optimization of this parameter thus require further investigation .

3.2 Flexural strength

The flexural strength results are presented in Fig. 5 and summarized in Table 2.

One-way ANOVA showed statistically significant differences between the groups tested for flexural strength ($F = 79.81$, $p < 0.05$) and surface roughness ($F = 48.75$, $p < 0.05$).

The highest flexural strength (105.86 MPa) was found for the samples of G7 and the lowest for the samples of G5 (35.46 MPa) and G6 (35.08 MPa), with statistically significant difference ($p < 0.001$, Tukey HSD post hoc test). The G7 group (PMMA block) also showed statistical difference, when compared to the groups of self-cured acrylic resins (G1-G4) and the group of heat-cured resins (G8). These PMMA blocks are polymerized under high pressure and temperature, without water interference and stored in environmental conditions where post-curing phenomena occur without interference, resulting in a compact structure with minimum porosity and improved physical properties [5,30–32].

There was no statistical difference between the groups of self-cured acrylic resins (G1-G4) and between the groups of photosensitive printing resins (G5 and G6). The flexural strength of groups G1 to G4 present values higher than those proposed by ISO ($\sigma > 60$ MPa). However, the addition of silanized silica NPs (s-SiO_2-NPs) in these groups adversely affected the flexural strength, diminishing slightly its value compared to the G1 control

group. The samples of G4, in which the largest amount of s-SiO_2-NPs was added (1.5 wt.%), showed the lowest flexural strength (67.55 MPa) among the self-curing resin groups, but yet not very different from groups G1, G2 and G3. The decrease in the mechanical strength is in agreement with the trend found in the literature, that the higher the filler content, the lower is the flexural strength [21,22,33,34]. The thermosetting resin group (G8), a material used for many years in dentistry, showed a high flexural strength (88.52 MPa, well beyond the minimum value recommended by ISO) and low surface roughness, acceptable by the standards recommended by Borchers and Bollen. In the groups G5 and G6, flexural strength was low (35.46 and 35.08 MPa, respectively), when compared to the other groups and the minimum ISO recommended value. Also in this case, no improvement of mechanical properties was found by the addition of NPs.

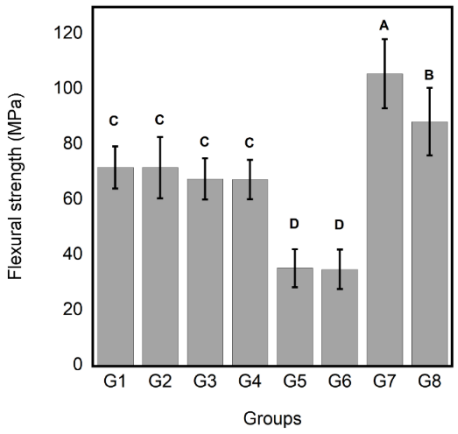

Fig. 5. Flexural strength for of sample from groups G1-G8. Different letters represent statistical difference at 5% level by Tukey's test.

4. Discussion

The surface roughness of intraoral materials such as self-curing acrylic resins and thermopolymerizable resins should be low to avoid plaque retention and consequently the development of periodontal diseases and the risk of caries. Surface morphology and roughness represent important properties of polymeric materials and originate from their chemical nature/structure and production processes.

In the case of self-curing resins, although SEM micrographs visually showed differences in the surface morphology between the samples with different NPs contents, the the roughness values showed a maximum increase of only 2.8 % in relation to the control sample. G3 and G4 samples, with a higher content of NPs in the composition, showed NPs scattered in the form of clusters. Cevik et. al. and Mussatto et. al. also observed caking effects on acrylic resins [22,34]. In the study by Mussatto et al., the groups in which silanized silica nanoparticles were added also showed a small increase in surface roughness when compared to the control [22]. This is an indication of better dispersion of the silanized particles in the acrylic resin, helping to achieve topographic uniformity. In the thermopolymerized resin samples (G8) no sign of porosity or voids was seen on the surface, probably due it longer polymerization cycle.

Although some of the nanocomposite resins presented adequate properties, for all different processing methods tested, no significant improvement in flexural strength were obtained by the addition of NPs. Insufficient dispersion and aggregation of the filler particles in the acrylic matrix have been pointed out as a cause of the adverse effect on flexural strength, as observed in Sodagar et al. and Mussatto et al. [21,22]. The time constraints imposed by the curing process makes optimization of dispersion procedures challenging since the initial setting of the self-curing process is fast (~ 5 min). Perhaps the nanoparticles can't finish dispersing as quickly as the setting time of the self-curing resin. Previous studies have also shown that flexural strength of provisional materials is impaired by water sorption, which results in a weakening resin matrix and by the release of unreacted monomers, degradation products, and leaching of filler ions, [21,22,34–36]. Hand-blended resins are also inherently porous, what favors air entrapment and water sorption, that can cause localized stresses when a load is applied [27]. Further studies regarding the optimization of NPs coating and interfacial interaction with the resin matrix are obviously needed.

In the case of 3D printing used in dentistry, it is important to improve the flexural strength of the resins, considering that most of 3D printers were not customized for dentistry. This may also partially explain the yet poor behavior of crowns or indirect resins printed Based on the results obtained in this study, 3D printing with photosensitive resins needs to improve flexural strength and surface roughness so that it can be useds in the

manufacture of crowns, veneers and indirect restorations with greater predictability of durability, especially in complex rehabilitations in patients with parafunctional habits. Tian et al. in his literature review on 3D printing reports that some factors can negatively affect the performance of 3D printed crowns and myorelaxing plates, such as word build angle and post-curing of the part causing inaccuracy and low flexural strength.[2,3,7]. In our case, the samples were printed in horizontal direction (0 degree build angle). Some papers reported that when the load is applied perpendicular to the printed layer, the compressive strength of the material is best [37–39]. Unkovskiy et. al. used stereolithography (SLA) and studied the effect of print orientation (0, 45 and 90 °), and found that the impression orientation influenced the accuracy. Specimens constructed with an orientation of 45° were found to be the most accurate [40]. The 90° specimens (layer orientation parallel to the axial load) showed superior flexural strength and flexural modulus. Park et al. printed prostheses with the DLP printer and also observed that when the print orientation was set to 45 or 60°, the fit of the part was optimized [41].

Another factor that can influence the mechanical properties of printed parts is the post-curing time [2,42–44]. In the study by Katheng et. al. the polymerization temperature had a greater effect than the polymerization time. Lower temperatures led to better dimensional accuracy and degree of polymerization of dentures printed with stereolithography (SLA) [44]. The parameters recommended by this study for post-curing parts printed by the SLA printer are 15 minutes and 40° C. In the present study DLP was used. The printed layer is cured in one direction and the post-curing process was performed in a 50W UV-light chamber for 10 min. A single post-cure time and exposure to a UV light (cold light) may be limiting factors in our study. Experiments to investigate the effect of light intensity and post-curing time and temperature on the mechanical behavior of the printed layers will be the subject of a subsequent work.

Clinically, the improvement in flexural strength has positive effects, such as greater durability in extensive temporary bridges that need to remain in use for long periods, especially in patients with parafunctional habits. These qualities are present in the samples performed with PMMA blocks (G7) and thermopolymerized resin (G8). However, the greater surface roughness of PMMA blocks (G7) could cause larger plaque accumulation and consequently periodontal diseases. Additional polishing can easily overcome this problem.

5. Conclusion

The incorporation of silanized silica nanoparticles into self-curing acrylic resins adversely affected the mechanical properties of the material, and the decrease of flexural strength may arise from poor dispersion of the filler. The PMMA block showed significantly higher flexural strength and is indicated for long term temporary prostheses provided surface roughness is diminished by extra polishing before delivery of the prosthesis. The thermopolymerizable resin showed excellent results with levels of surface roughness and flexural strength better than what is recommended by ISO. Thermally cured resin, therefore, remains the gold standard for these properties. The photosensitive resin for 3D printing was the material that showed the lowest flexural strength, even after the incorporation of the silica NPs. There is a worldwide trend to incorporate 3D printing technology into everyday dental practice. It is believed that the main challenge for the escalation of 3D printing in dentistry concerns the resins used in printing. Thus there is room for further improvement of mechanical properties these resins especially when prostheses, crowns, myorelaxing plates will be used in complex cases of rehabilitation in patients with parafunctional habits for long periods. Therefore, in vitro studies on the incorporation of nanometric filler particles in resins used for 3D printing and in self-polymerizing resins need continue to improve mechanical properties as flexural strength and surface roughness.

6. References

[1] Costa LPG da, Zamalloa SID, Alves FAM, Spigolon R, Mano LY, Costa C, et al. 3D printers in dentistry: a review of additive manufacturing techniques and materials. Clin Lab Res Dent 2021:1–10. https://doi.org/10.11606/issn.2357-8041.clrd.2021.188502.

[2] Tian Y, Chen C, Xu X, Wang J, Hou X, Li K, et al. A Review of 3D Printing in Dentistry: Technologies, Affecting Factors, and Applications. Scanning 2021;2021:1–19. https://doi.org/10.1155/2021/9950131.

[3] Kessler A, Hickel R, Reymus M. 3D Printing in Dentistry—State of the Art. Oper Dent 2020;45:30–40. https://doi.org/10.2341/18-229-L.

[4] Alghazzawi TF. Advancements in CAD/CAM technology: Options for practical implementation. J Prosthodont Res 2016;60:72–84. https://doi.org/10.1016/j.jpor.2016.01.003.

[5] Alp G, Murat S, Yilmaz B. Comparison of Flexural Strength of Different CAD/CAM PMMA-Based Polymers. J Prosthodont 2019;28:e491–5. https://doi.org/10.1111/jopr.12755.

[6] Lourinho C, Salgado H, Correia A, Fonseca P. Mechanical Properties of Polymethyl Methacrylate as Denture Base Material: Heat-Polymerized vs. 3D-Printed—Systematic Review and Meta-Analysis of In Vitro Studies. Biomedicines 2022;10:2565. https://doi.org/10.3390/biomedicines10102565.

[7] Cai H, Xu X, Lu X, Zhao M, Jia Q, Jiang H-B, et al. Dental Materials Applied to 3D and 4D Printing Technologies: A Review. Polymers (Basel) 2023;15:2405. https://doi.org/10.3390/polym15102405.
[8] Tsoukala E, Lyros I, Tsolakis AI, Maroulakos MP, Tsolakis IA. Direct 3D-Printed Orthodontic Retainers. A Systematic Review. Children 2023;10:676. https://doi.org/10.3390/children10040676.
[9] Huang S, Wei H, Li D. Additive manufacturing technologies in the oral implant clinic: A review of current applications and progress. Front Bioeng Biotechnol 2023;11. https://doi.org/10.3389/fbioe.2023.1100155.
[10] Raszewski Z. Acrylic resins in the CAD/CAM technology: A systematic literature review. Dent Med Probl 2020;57:449–54. https://doi.org/10.17219/dmp/124697.
[11] Miura S, Fujisawa M. Current status and perspective of CAD/CAM-produced resin composite crowns: a review of clinical effectiveness. Jpn Dent Sci Rev 2020;56:184–9. https://doi.org/10.1016/j.jdsr.2020.10.002.
[12] Jovanović M, Živić M, Milosavljević M. A potential application of materials based on a polymer and CAD/CAM composite resins in prosthetic dentistry. J Prosthodont Res 2021;65:137–47. https://doi.org/10.2186/jpr.JPOR_2019_404.
[13] Stansbury JW, Idacavage MJ. 3D printing with polymers: Challenges among expanding options and opportunities. Dent Mater 2016;32:54–64. https://doi.org/10.1016/j.dental.2015.09.018.
[14] Prpic V, Slacanin I, Schauperl Z, Catic A, Dulcic N, Cimic S. A study of the flexural strength and surface hardness of different materials and technologies for occlusal device fabrication. J Prosthet Dent 2019;121:955–9. https://doi.org/10.1016/j.prosdent.2018.09.022.
[15] Xu X, He L, Zhu B, Li J, Li J. Advances in polymeric materials for dental applications. Polym Chem 2017;8:807–23. https://doi.org/10.1039/C6PY01957A.
[16] AlKahtani RN. The implications and applications of nanotechnology in dentistry: A review. Saudi Dent J 2018;30:107–16. https://doi.org/10.1016/j.sdentj.2018.01.002.
[17] Alshamrani A, Alhotan A, Kelly E, Ellakwa A. Mechanical and Biocompatibility Properties of 3D-Printed Dental Resin Reinforced with Glass Silica and Zirconia Nanoparticles: In Vitro Study. Polymers (Basel) 2023;15:2523. https://doi.org/10.3390/polym15112523.
[18] Wang J, Jiang W, Liang J, Ran S. Influence of silver nanoparticles on the resin-dentin bond strength and antibacterial activity of a self-etch adhesive system. J Prosthet Dent 2022;128:1363.e1-1363.e10. https://doi.org/10.1016/j.prosdent.2022.09.015.
[19] Yao S, Qin L, Wang Z, Zhu L, Zhou C, Wu J. Novel nanoparticle-modified multifunctional microcapsules with self-healing and antibacterial activities for dental applications. Dent Mater 2022;38:1301–15. https://doi.org/10.1016/j.dental.2022.06.012.
[20] Sears LM, Wu L, Morrow BR, Hollis W, Cagna DR, Hong L. Effects of NanoAg-ACP Microparticles as Bioactive Fillers on the Mechanical and Remineralization Properties of Dental Resin Cement. J Prosthodont 2022;31:705–13. https://doi.org/10.1111/jopr.13473.
[21] Sodagar A, Bahador A, Khalil S, Saffar Shahroudi A, Zaman Kassaee M. The effect of TiO2 and SiO2 nanoparticles on flexural strength of poly (methyl methacrylate) acrylic resins. J Prosthodont Res 2013;57:15–9. https://doi.org/10.1016/j.jpor.2012.05.001.
[22] Mussatto CMB, Oliveira EMN, Subramani K, Papaléo RM, Mota EG. Effect of silica nanoparticles on mechanical properties of self-cured acrylic resin. J Nanoparticle Res 2020;22:317. https://doi.org/10.1007/s11051-020-05050-y.
[23] MOHSEN NM, CRAIG RG. Effect of silanation of fillers on their dispersability by monomer systems. J Oral Rehabil 1995;22:183–9. https://doi.org/10.1111/j.1365-2842.1995.tb01562.x.
[24] Naveen KS, Singh JP, Viswambaran M, Dhiman RK. Evaluation of flexural strength of resin interim restorations impregnated with various types of silane treated and untreated glass fibres. Med J Armed Forces India 2015;71:S293–8. https://doi.org/10.1016/j.mjafi.2012.06.015.
[25] Sideridou ID, Karabela MM. Effect of the amount of 3-methacyloxypropyltrimethoxysilane coupling agent on physical properties of dental resin nanocomposites. Dent Mater 2009;25:1315–24. https://doi.org/10.1016/j.dental.2009.03.016.
[26] Karabela M, Siderou I. Effect of the structure of silane coupling agent on sorption characteristics of solvents by dental resin-nanocomposites. Dent Mater 2008;24:1631–9. https://doi.org/10.1016/j.dental.2008.02.021.
[27] 20795-1:2013 I. Dentistry — Base polymers — Part 1: Denture base polymers, 2013. https://doi.org/11.060.10.
[28] Borchers L, Tavassol F, Tschernitschek H. Surface quality achieved by polishing and by varnishing of temporary crown and fixed partial denture resins. J Prosthet Dent 1999;82:550–6. https://doi.org/10.1016/S0022-3913(99)70053-3.
[29] Bollenl CML, Lambrechts P, Quirynen M. Comparison of surface roughness of oral hard materials to the threshold surface roughness for bacterial plaque retention: A review of the literature. Dent Mater 1997;13:258–69. https://doi.org/10.1016/S0109-5641(97)80038-3.
[30] Alt V, Hannig M, Wöstmann B, Balkenhol M. Fracture strength of temporary fixed partial dentures:

CAD/CAM versus directly fabricated restorations. Dent Mater 2011;27:339–47. https://doi.org/10.1016/j.dental.2010.11.012.
[31] Yao J, Li J, Wang Y, Huang H. Comparison of the flexural strength and marginal accuracy of traditional and CAD/CAM interim materials before and after thermal cycling. J Prosthet Dent 2014;112:649–57. https://doi.org/10.1016/j.prosdent.2014.01.012.
[32] Liebermann A, Wimmer T, Schmidlin PR, Scherer H, Löffler P, Roos M, et al. Physicomechanical characterization of polyetheretherketone and current esthetic dental CAD/CAM polymers after aging in different storage media. J Prosthet Dent 2016;115:321-328.e2. https://doi.org/10.1016/j.prosdent.2015.09.004.
[33] Balos S, Pilic B, Markovic D, Pavlicevic J, Luzanin O. Poly(methyl-methacrylate) nanocomposites with low silica addition. J Prosthet Dent 2014;111:327–34. https://doi.org/10.1016/j.prosdent.2013.06.021.
[34] Cevik P, Yildirim-Bicer AZ. The Effect of Silica and Prepolymer Nanoparticles on the Mechanical Properties of Denture Base Acrylic Resin. J Prosthodont 2018;27:763–70. https://doi.org/10.1111/jopr.12573.
[35] Nazirkar G, Bhanushali S, Singh S, Pattanaik B, Raj N. Effect of Anatase Titanium Dioxide Nanoparticles on the Flexural Strength of Heat Cured Poly Methyl Methacrylate Resins: An In-Vitro Study. J Indian Prosthodont Soc 2014;14:144–9. https://doi.org/10.1007/s13191-014-0385-8.
[36] Wang R, Tao J, Yu B, Dai L. Characterization of multiwalled carbon nanotube-polymethyl methacrylate composite resins as denture base materials. J Prosthet Dent 2014;111:318–26. https://doi.org/10.1016/j.prosdent.2013.07.017.
[37] Chockalingam K, Jawahar N, Chandrasekhar U. Influence of layer thickness on mechanical properties in stereolithography. Rapid Prototyp J 2006;12:106–13. https://doi.org/10.1108/13552540610652456.
[38] Chockalingam K, Jawahar N, Chandrasekar U, Ramanathan KN. Establishment of process model for part strength in stereolithography. J Mater Process Technol 2008;208:348–65. https://doi.org/10.1016/j.jmatprotec.2007.12.144.
[39] Alharbi N, Alharbi S, Cuijpers VMJI, Osman RB, Wismeijer D. Three-dimensional evaluation of marginal and internal fit of 3D-printed interim restorations fabricated on different finish line designs. J Prosthodont Res 2018;62:218–26. https://doi.org/10.1016/j.jpor.2017.09.002.
[40] Unkovskiy A, Bui PH-B, Schille C, Geis-Gerstorfer J, Huettig F, Spintzyk S. Objects build orientation, positioning, and curing influence dimensional accuracy and flexural properties of stereolithographically printed resin. Dent Mater 2018;34:e324–33. https://doi.org/10.1016/j.dental.2018.09.011.
[41] Park G-S, Kim S-K, Heo S-J, Koak J-Y, Seo D-G. Effects of Printing Parameters on the Fit of Implant-Supported 3D Printing Resin Prosthetics. Materials (Basel) 2019;12:2533. https://doi.org/10.3390/ma12162533.
[42] Cheah CM, Fuh JYH, Nee AYC, Lu L. Mechanical characteristics of fiber-filled photo-polymer used in stereolithography. Rapid Prototyp J 1999;5:112–9. https://doi.org/10.1108/13552549910278937.
[43] Jindal P, Juneja M, Bajaj D, Siena FL, Breedon P. Effects of post-curing conditions on mechanical properties of 3D printed clear dental aligners. Rapid Prototyp J 2020;26:1337–44. https://doi.org/10.1108/RPJ-04-2019-0118.
[44] Katheng A, Kanazawa M, Iwaki M, Minakuchi S. Evaluation of dimensional accuracy and degree of polymerization of stereolithography photopolymer resin under different postpolymerization conditions: An in vitro study. J Prosthet Dent 2021;125:695–702. https://doi.org/10.1016/j.prosdent.2020.02.023.